**Research Article**

# Rapid Adaptation of Cellular Metabolic Rate to the microRNA Complements of Mammals

Bastian Fromm, PhD
The Arctic University Museum of Norway
UiT- The Arctic University of Norway
9037 Tromsø, Norway

and

Thomas Sorger, PhD*
Department of Biology
Roger Williams University
Bristol, Rhode Island 02809, USA

* corresponding author

## ABSTRACT

Terrestrial mammals range over six orders of magnitude in size, while average cellular, or specific metabolic rate *(sMR*) varies only ~5-fold, constrained by the strict matching of protein synthesis to cell size. Protein synthesis, the single most costly metabolic activity, accounts for 20% of ATP turnover, and the speed of translation can be increased only at the expense of increased energy dissipation due to misreading errors and stochastic translation noise. We hypothesized that global microRNA activity evolved under the same constraints as *sMR* and would therefore exhibit a similar pattern of variation. This expectation was met by the number of microRNA families: based on the manually curated microRNA gene database MirGeneDB, the acquisition of microRNA families (*mirFam*) accelerated two-fold in late-branching mammals with body temperatures ($T_b$) > 36°C, relative to early-branching mammals ($T_b$ < 36°C), independent of phylogenetic distance. When *sMR* is fit to *mirFam* by maximum likelihood, the variation is homoscedastic, allowing us to compare models for the evolution of *sMR* in relation to *mirFam*. With *mirFam* as the predictor, an Ornstein-Uhlenbeck (OU) process of stabilizing selection accounted better for the biphasic evolution of *sMR* than did the corresponding Brownian motion model, and was optimized when *sMR* was scaled to $M^{0.75}$. OU simulations with an adaptive shift at the divergence of Boreoeutheria predicted 95% of the variation in *sMR*. We infer that the advent of placentation led to the emergence of an adaptive optimum characterized by higher body temperatures, faster *MR*s, and heightened global microRNA activity.

## INTRODUCTION

Among the ancestors of mammalian crown species, resting metabolic rate (*rMR*) and body mass evolved in tandem according to a strongly conserved allometry (Kleiber, 1932; Brody and Proctor, 1932; Savage et al, 2004; White et al, 2006; McNab, 2008; McNab, 2009; Naya et al, 2013; Gillooly et al, 2017; Ballesteros et al, 2018; McNab, 2019); as a result, the ratio of *MR*/*M* , or specific *MR* (*sMR*) has been highly constrained (White et al, 2019 and Supplementary Figure 1). Since cellular *MR* accounts for 90% of *sMR* (Rolfe and Brown, 1997), the $10^6$-fold range in the mass of terrestrial mammals represents, to a first approximation, variation in the total number of cells with highly constrained cell size and cellular *MR*.

One strong constraint on cellular *MR* is the cell cycle-related coupling of macromolecular synthesis and cell size in mammalian cells, as in yeast cells (Ginzberg et al, 2018; Knapp et al, 2019; Neurohr et al, 2019) (for reviews, see Björklund, 2019 and Zatulovskiy and Skotheim, 2020). Protein synthesis drives 20% of ATP turnover and is the single most costly metabolic process in mammalian cells (Rolfe and Brown, 1997). The efficiency of protein synthesis can be expected to impact evolutionary fitness directly, by determining the minimum daily energy requirement, as well as indirectly, by affecting the trade-off between energy flows to somatic maintenance, reproductive reserves, and parental care (Maino et al, 2014; Swanson et al, 201; Koteja, 2000). Since the radiation of mammals to different climatic niches depended on the coordinated evolution of mass, *MR* and thermal conductance (Scholander et al, 1950; Porter & Kearney, 2009; Fristoe

et al, 2015; Clavel and Morlon, 2017), a decrease in cellular metabolic efficiency *per se* would have negatively impacted fitness by raising the rate of heat dissipation (Porter & Kearney, 2009; Ballesteros et al, 2018), and also thereby limiting maximal *MR* (Speakman and Krol, 2010).

Matching of the rate of protein synthesis to cell size has been predicted by models in which the rate of translation in exponentially growing cells is limited by competition among mRNAs for ribosomes (Kafri et al, 2016; Lin and Amir, 2018). A slow rate of translation relative to transcription also minimizes both translation noise (Ozbudak et al, 2002; Lin and Amir, 2021) and energy losses to error correction by kinetic proofreading (Hopfield, 1974; Ninio, 1975; Bennett, 1979; Barato and Seifert, 2015; Banerjee et al, 2017; Mallory et al, 2019; Yu et al, 2022). These adaptations can be understood in light of the 10- to 100-fold higher thermodynamic cost per gene of translation relative to transcription in eukaryotes (Wagner, 2005; Lynch and Marinov, 2015).

Absent the evolution of compensatory mechanisms, the fitness benefits associated with higher mammalian $T_b$'s and cellular *MR*s would have been offset by increasingly noisy and error-prone translation. MicroRNAs are post-transcriptional regulators that can attenuate intrinsic translation noise (Bartel and Chen, 2004; Hornstein and Shomron, 2006; Schmiedel et al, 2015; Bartel, 2018). Unlike other regulators of gene expression, global microRNA activity has an obligatory effect on *sMR* by decreasing the overall rate of translation (Krek et al, 2005; Baek et al, 2008; Selbach et al, 2008; Friedman et al, 2009). Changes in the rate of translation exert a disproportionate effect on *sMR*, since protein synthesis is the single least efficient, as well as most costly, cellular metabolic process (Rolfe and Brown, 1997). Assuming conservatively that combinatorial global microRNA activity reduces the average rate of translation by 25% (Krek et al, 2005; Baek et al, 2008; Selbach et al, 2008; Schmiedel et al, 2015), a 10-fold increase in cellular *MR*, without a corresponding increase in global microRNA activity, would incur an estimated 4.5% loss of metabolic efficiency due to protein overproduction. (While not directly comparable, it is worth noting that losses of fitness of up to 3% were found when the translation noise of individual, constitutive proteins in yeast was doubled: Schmiedel et al, 2019.)

Indeed, the rates of translation of low- and high-abundance transcripts conform to the predicted outcome of global microRNA activity and appear to have evolved under an energy constraint (Vogel et al, 2010; Schwanhäusser et al, 2011): microRNAs preferentially repress low-abundance transcripts (Bartel and Chen, 2004; Schmiedel et al, 2015), which are more costly to translate than highly abundant mRNAs (Schwanhäusser et al, 2011), such as those encoded by housekeeping genes. Assuming such a constraint on energy efficiency, we postulated that suppression of stochastic expression noise by global microRNA activity varied directly with cellular *MR* as higher $T_b$'s evolved among late-branching mammalian lineages.

Exhaustive sequencing and genome curation have revealed that the number of families of conserved, microRNA-encoding genes has grown steadily over the course of vertebrate evolution, with very low rates of loss (Fromm et al, 2015; Tarver et al, 2018; Fromm et al, 2020; Fromm et al, 2021). The acquisition of shared microRNA families (*mirFam*) accelerated in placental mammals (Fromm et al, 2020) while, based on the number of predicted 3'-UTR microRNA binding sites, the average number of potential microRNA targets per coding gene increased approximately fourfold, from 1.87 in the opossum to 3.84 in the mouse to 7.08 in humans (Agarwal et al, 2015). The acceleration of *mirFam* acquisition coincided closely with an elevation in $T_b$ and *MR* among those mammalian orders that diverged more recently than Chiroptera: of the six mammalian orders with $T_b$'s significantly higher than Chiroptera, only one (Macroscelidea) diverged earlier than Chiroptera; conversely, of the ten orders with lower average $T_b$'s, only one (Pholidota) diverged later than Chiroptera (Clarke et al, 2010) (Supplementary Figure S2). Thus, the size of the microRNA repertoire in mammals has varied in parallel with cellular *MR* and therefore with the overall translation rate, as predicted for global microRNA activity.

Given the dependence of cellular *MR* on the rate of protein synthesis, we asked whether the strong correlation between *sMR* and *mirFam* better reflected phylogenetic distance (Brownian motion model), or the outcome of stabilizing selection (Ornstein-Uhlenbeck model) (Bartoszek et al, 2012). Second, we asked at which stage of mammalian evolution an adaptive shift would have been most likely to replicate the biphasic increases in *sMR* and *mirFam*.

## RESULTS

### *Allometric scaling of vertebrate MRs by maximum likelihood*

We first established that our sample of 20 vertebrate species in MirGeneDB was broadly representative of vertebrates with respect to the distribution of *rMR*. Conventional studies of the evolution of metabolic rate have addressed constraints on the whole animal, such as mass, temperature, aridity, and diet, with the effect of each constraint inferred by residual analysis of the regression of log *rMR* on log mass (see, for example, Kleiber, 1932; McNab, 2008; McNab, 2009; Naya et al, 2013; Ballesteros et al, 2018; McNab, 2019). As shown in Figure 1A, the *rMR*s of the 14 endotherms and 6 ectotherms exhibited a conserved relationship to mass, with slopes (0.75 and 0.88 respectively) very similar to those reported in previous, large-scale studies (White et al, 2006; Gillooly et al, 2017).

In order to analyze how *sMR* varies in relation to *mirFam*, we used a maximum likelihood approach (White, 2011) to find the optimal allometric transformation ($rMR/M^{exp} = sMR$) with respect to *mirFam* (or other normally distributed covariate). For example, maximum likelihood scaling of the metabolic rates of the 20 vertebrates in this study (with resolution $M^{0.1}$) yielded a single optimal slope for both ectotherms and endotherms of $rMR/M^{0.80}$ (hereafter *sMR*80), with normally distributed residuals and a smaller residual error than the log-based method for either endotherms or ectotherms ($R^2$ = 0.9996, $P$ =

6.36e-32) (Figure 1B). When maximum likelihood is applied to the scaling of *sMR* in order to match the distribution of a third variable, such as *mirFam*, the variation is homoscedastic and appropriate for comparing the evolutionary rates of species ranging in size over several orders of magnitude (Benson et al, 2022) (Figure 3 and Supplementary Figure S3).

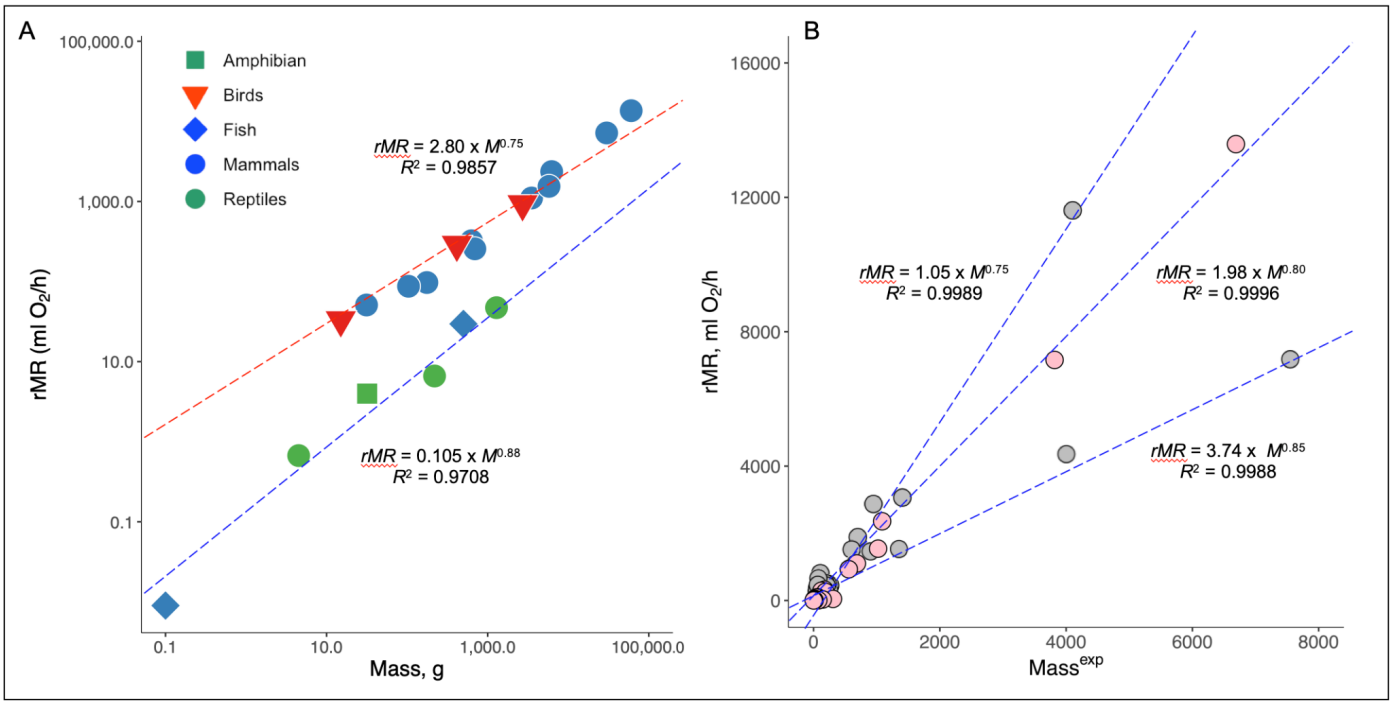


**Figure 1**. Comparison of the allometric scaling of the *sMR*s of 20 vertebrates by (A) the conventional power law method, or (B) maximum likelihood scaling according to the optimal fit ($M^{0.80}$) and two suboptimal fits ($M^{0.75}$, $M^{0.85}$).

### *The acquisition of microRNA families accelerated in late-branching mammals*

The number of families of conserved, microRNA-encoding genes has increased steadily in the order of divergence of vertebrate clades, except among Archosauria (Figure 2A). The variation in *mirFam* was unrelated to genome size or number of coding genes (Supplementary Table S2), but was 87% correlated with *sMR* ($rMR/M^{0.80}$) across 16 non-avian vertebrates ($P$ = 2.20e-16, Spearman rank correlation) (Figure 2B). The acquisition of shared microRNA families accelerated in placental mammals, with increases of 46 in the 64 million years between the divergences of Theria and Placentalia, and 27 in the 8.7 million years between the divergence of Atlantogenata and Euarchontoglires (Álvarez-Carretero et al, 2022). Among the latter, fewer than ten microRNA families are uniquely expressed in the placenta (Fromm et al, 2020). These differences correspond to gains of 0.92% per million years in pre-placental mammals *versus* 2.24% per million years among placental mammals (Fromm et al, 2020; Álvarez-Carretero et al, 2022). Consequently, the number of microRNA families common to all Euarchontoglires (154), as well the number of genes, is approximately twice the number shared by all Theria (81) (Figure 2A, Supplementary Table S1) (Fromm et al, 2020).

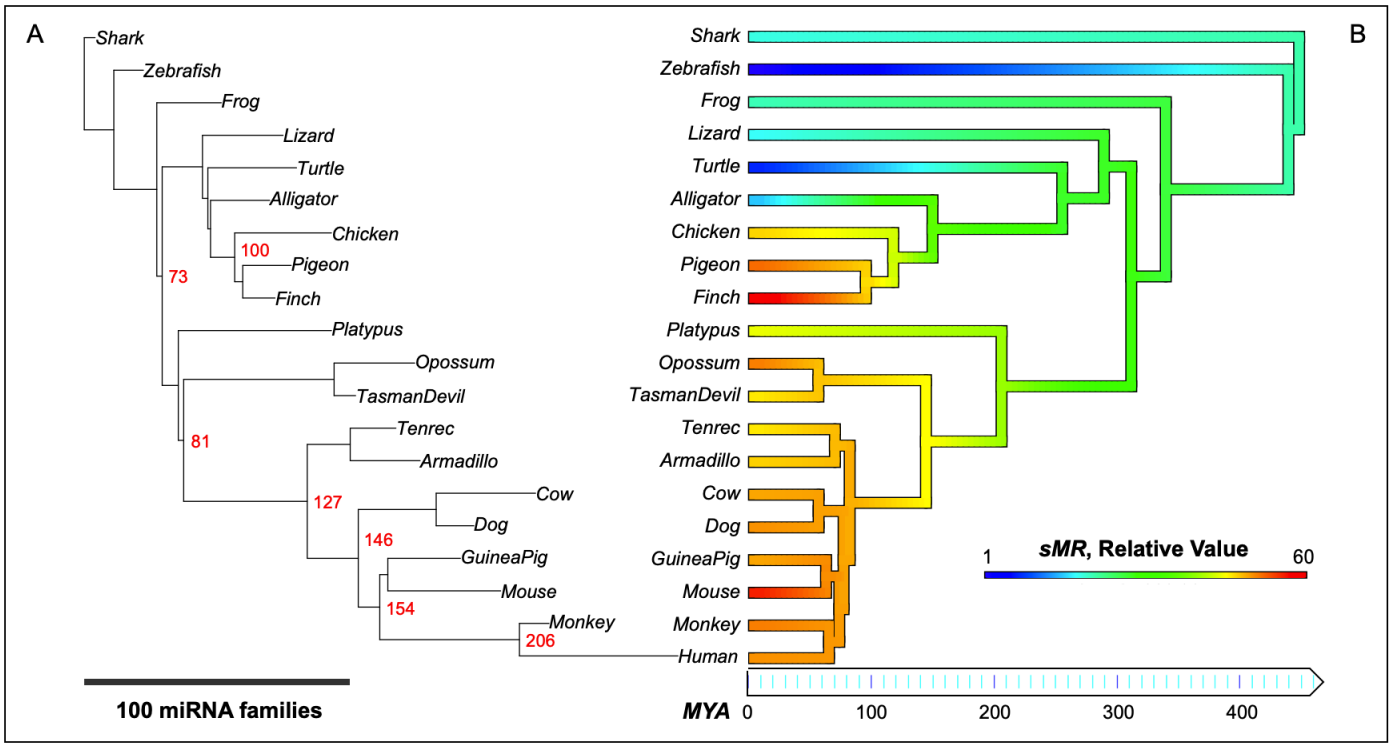


**Figure 2**. Evolution of the number of microRNA families and average cellular or specific *MR* (*sMR*).
A. Distance tree of microRNA families. Branch lengths represent the total number of families. Node values represent the number of shared microRNA families in each clade.
B. The log ratios of *sMR*s ($rMR/M^{0.80}$) were scaled to the original range of *sMR* and mapped onto the vertebrate phylogeny. Divergence times were drawn from Álvarez-Carretero et al 2022) for mammals, and Irisarri et al (2017) for earlier-branching vertebrates.

### *Tetrapod sMRs are correlated with mirFam independent of phylogenetic distance*

Phylogenetic linear regression indicated that the number of microRNA families in 14 non-avian tetrapods accounted for 84% of the variation in optimally scaled *sMR* ($rMR/M^{0.68}$, $P$ = 2.26e-06) (Figure 3A), independent of phylogenetic distance (Pagel's *lambda* = 0.00). The variation with respect to the number of microRNA genes was weaker and secondary to phylogeny (Pagel's *lambda* = 1.0). Similar results were obtained when only mammals were considered, with the optimal allometric exponent shifting from 0.68 to 0.71, consistent with the higher range of body mass (Supplementary Table S2).

The previous analysis excluded the three bird species in our sample (chicken and two flying birds) since the absolute number of avian microRNA families decreases in phylogenetic order (Figure 2A) (Supplementary Table S1). In large datasets, the overall *MR* of birds exhibits a markedly lower (log-based) allometric exponent than that of mammals, *e.g.* $M^{0.64}$ *versus* $M^{0.73}$ (Fristoe et al, 2015; Ballesteros et al, 2018). When scaled to $M^{0.64}$, the slope of the regression of the bird *sMRs* on *mirFam* was 0.00 (Figure 3B), and turned positive for any allometric exponent < 0.64. That is, when scaled with an allometric exponent < 0.64, bird *sMR*s vary positively with *mirFam*. As it is in mammals, the optimal

allometric scaling of *sMR* with respect to *mirFam* in birds may be displaced toward a greater dependence on surface area *i.e.* lower allometric exponent, than for the dependence of *rMR* on mass.

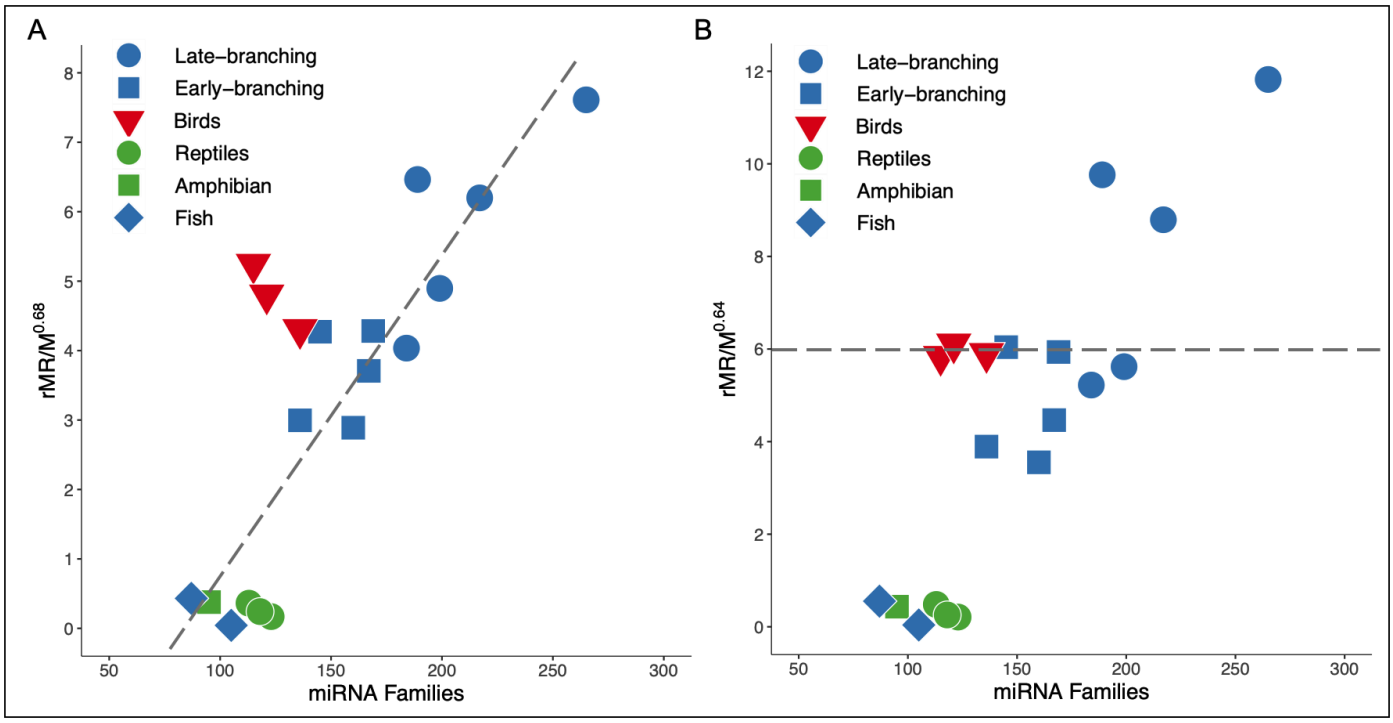


**Figure 3**. Phylogenetic regression of specific *MR* on the number of microRNA families.
A. The number of microRNA families in non-avian tetrapods accounted for 84% of the variation in *sMR*68, independent of phylogenetic distance (Supplementary Table S2).
B. The same data scaled to the slope of log rMR/log mass (0.64) in 211 birds (Fristoe et al, 2015).

### *The biphasic evolution of sMR conforms to stabilizing selection with respect to mirFam*

We compared two hypotheses for the evolution of metabolic rates in relation to the microRNA complement: a Brownian motion (BM) process, where *sMRs* diverge to in proportion to phylogenetic distance, *versus* an Ornstein-Uhlenbeck (OU) process, according to which *sMR*s, under the influence of stabilizing selection, converge asymptotically toward the distribution of an independently varying predictor (Bartoszek et al, 2012), in this case, the number of microRNA families. We applied two complementary methods in order to test these models: first, we compared how well each process fit the *sMR-mirFam* relationship across the range of allometric exponents 0.66 - 0.80; second, using the same phylogeny and *mirFam* distribution, we developed BM and OU simulations that optimized the correlation with the actual distribution of *sMR* values.

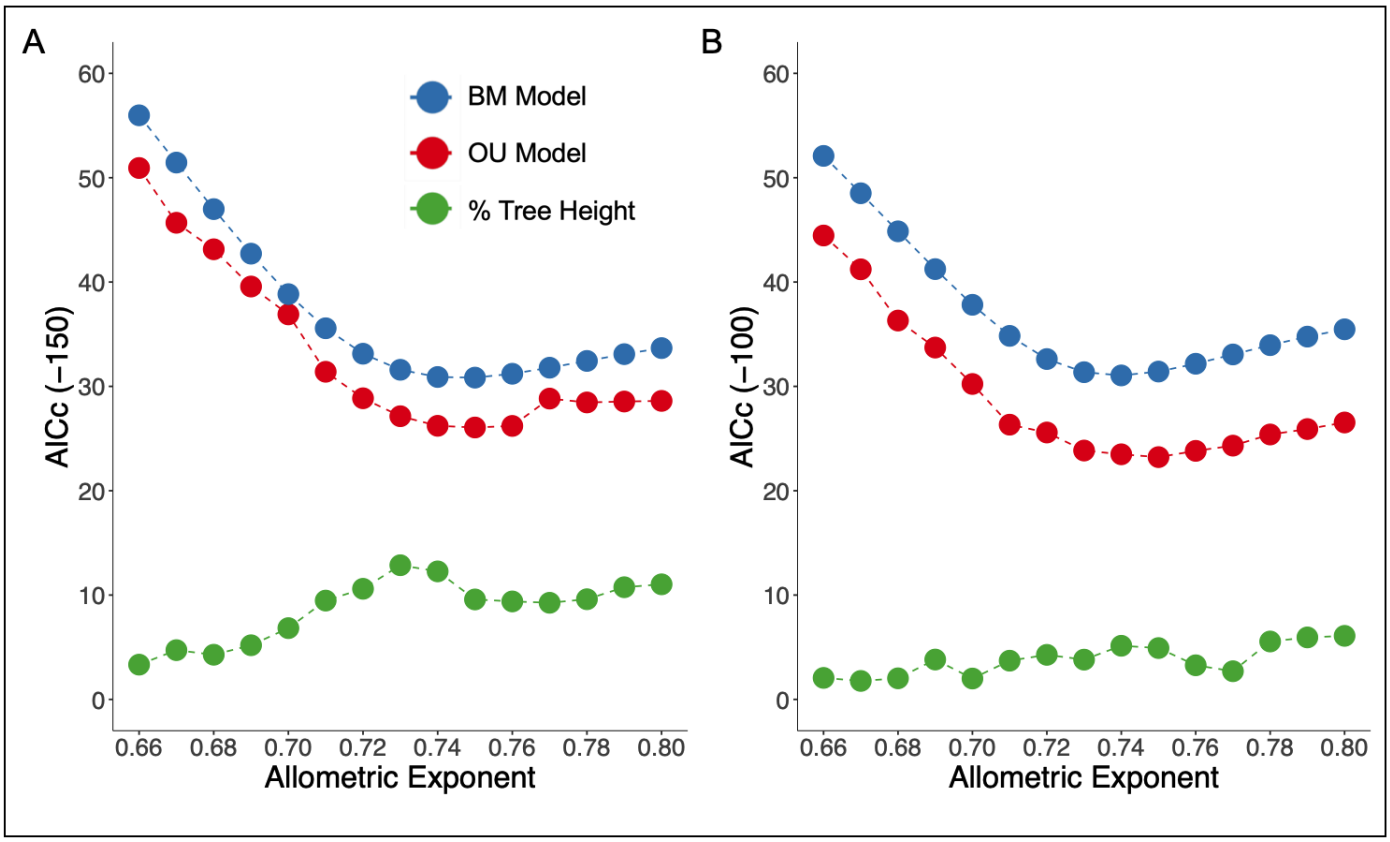


**Figure 4**. Comparison of BM and OU models for the variation of s*MR* with respect to the number of microRNA families across 14 tetrapods (A) or 10 mammals (B). Curves represent the corrected values of the Akaike information criterion (AICc) for each model, and the rate of adaptation (% tree height) for the OU models. Note the difference in scaling of the ordinates.

For any *MR* scaling in the range $M^{0.66}$ - $M^{0.80}$, the BM model for the evolution of *sMR* with respect to *mirFam* was inferior to the OU model (Figure 4A): at $M^{0.75}$, the ΔAICc (BM-OU) value was +2.68 before correction, and +6.88 after empirical correction of the bias recorded in 40 OU and 40 BM simulations on the same phylogenetic tree (Supplementary Table S3). The inferred rate of adaptation of *sMR* with respect to *miFam* at $M^{0.75}$ corresponded to 12.63% of the tetrapod tree (Figure 4A), or 4.92% when only the 10-mammal tree was considered (Figure 4B). Specific *MR*s exhibited a similar optimum with respect to the number of microRNA genes (*mirGen*), albeit with smaller differences in the AICc criterion between the OU and BM models (Supplementary Figure S4). However, in models of *sMR* variation in relation to genome size (*Gnm*) or number of coding genes (*Cdg*), no such inflection was observed, and AICc values declined monotonically (Supplementary Figure S4).

We then simulated the evolution of *sMR* with respect to *mirFam* in 14 tetrapods, by either a BM or OU process assuming two adaptive shifts: the first first shift corresponds to the divergence of mammals, while the second shift corresponds to the divergence of either Placentalia, Boreoeutheria, or Euarchontoglires (Figure 5A) (Bastide et al, 2018).

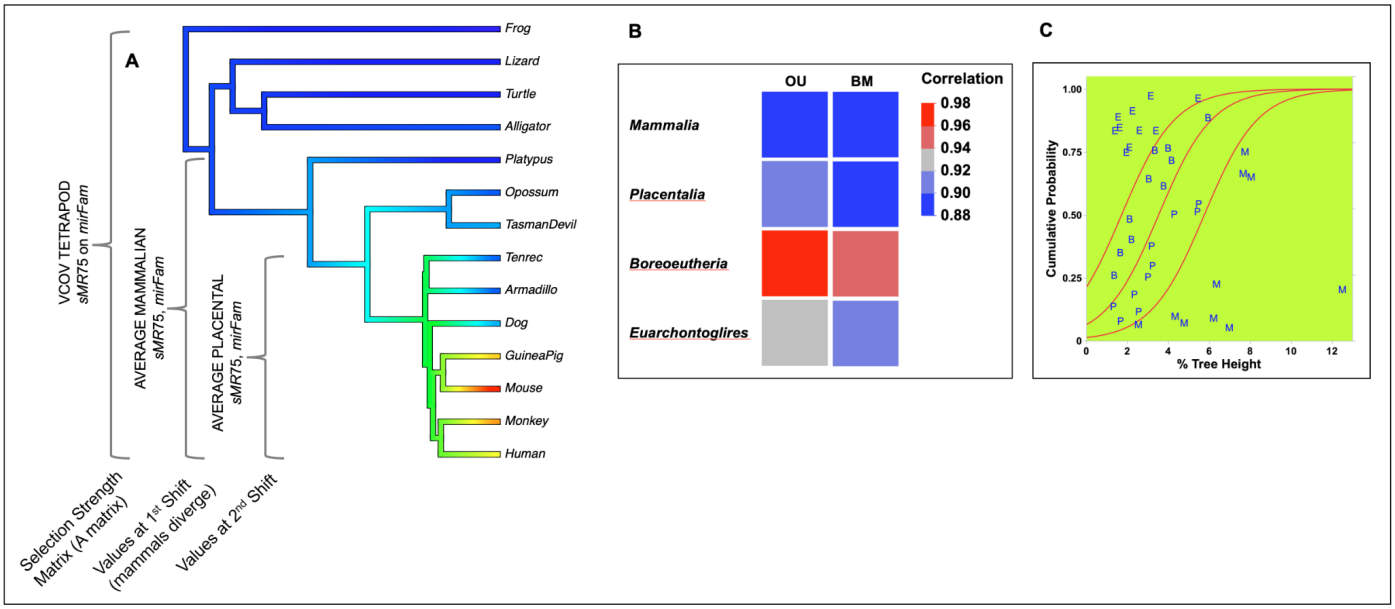


**Figure 5**. Design and analysis of simulated adaptive shifts in the evolution of *sMR* relative to *mirFam*. A. The variance/covariance matrix for the regression of *sMR*75 on *mirFam* was used as the selection strength matrix to generate pairs of values for these traits. The average values of these traits across all mammals, or across placental mammals, were assigned to the first shift (divergence of mammals) and second shift, respectively. Phenogram colors correspond to the log of the *sMR*75 values scaled to the original, 36-fold range. B. Correlations with the actual *sMR*75 distribution of the average of ten simulations of the OU or BM process in 14 tetrapods. Adaptive shifts were modeled at the divergence of Mammalia (single shift), with a second shift at the divergence of either Placentalia, Boreoeutheria or Euarchontoglires ($P$ = 1.23e-05 for OU *versus* BM, Boreoeutheria shift). C. Validation of the estimated rates of adaptation: prediction of shift positions according to the % tree height obtained from ten OU models. Shift positions are indicated by the first letter of each diverging clade (M, P, B, E). $P$ = 5.19e-06 (ordinal logistic regression).

OU and BM models simulated the biphasic evolution of *sMR* in mammals most precisely when this was scaled to $M^{0.75}$ (Supplementary Figure S5). An OU model with an adaptive shift at the divergence of Boreoeutheria accounted for 95% of the variation in *sMR*75 ($P$ = 4.10e-09), compared to 88% for the corresponding BM model (Figure 5B). Estimates of the rate of adaptation increased in the order of the phylogenetic position of the second adaptive shift, corresponding to decreasing distance from the tips of the phylogenetic tree ($P$ = 5.19e-06, ordinal logistic regression) (Figure 5C).

In sum, for both OU and BM models of the variation in *sMR* across mammals, the optimal allometric scaling with respect to *mirFam* corresponds closely to the conserved three-quarter power law model for the overall dependence of *rMR* on mass. It remains to be determined whether in birds, by analogy, evolutionary models of *sMR* variation in relation to *mirFam* exhibit optimal scaling corresponding to the conserved ~ ⅔ power law model for avian metabolic rates (Fristoe et al, 2015; Ballesteros et al, 2018).

## DISCUSSION

### *MirGeneDB is a new reference for comparative biology research.*

Given the impact of overall microRNA activity on the total rate of translation, we hypothesized that global microRNA activity in mammals evolved under the same constraints as cellular *MR* (*sMR*), and would therefore exhibit a similar pattern of variation. The covariation that we have demonstrated between *mirFam* and *sMR* is consistent with the assumption that *mirFam* is a useful proxy for global microRNA activity. Previous comparative studies have referenced molecular traits, such as genome size, the number of protein-coding genes, or quantity of non-coding DNA (see, for example, Choi et al, 2020). With the availability of the manually curated microRNA gene database, MirGeneDB, we are able to extend this approach to conserved microRNA families and genes in a wide range of vertebrate species and organs (Fromm et al, 2020; Fromm et al, 2021).

A major concern in microRNA research in the past has been the quality of the online repository miRBase. This database contains many false-positives while at the same time missing a large number of *bona fide* microRNAs from undersampled species, which were misinterpreted as secondary losses (Chiang et al, 2010; Langenberger et al, 2011; Wang and Liu, 2011; Jones-Rhoades, 2012; Meng et al, 2012; Tarver et al, 2013; Castellano and Stebbing, 2013; Taylor et al, 2014; Fromm et al, 2015; Ludwig et al, 2017; Axtell et al, 2018; Fromm et al, 2020). Consequently, the conservation and utility of microRNAs as phylogenetic markers was questioned in the past (Thompson et al, 2014). However, these omissions were clearly technical artifacts, since losses of microRNA families have rarely been observed in well-annotated repertoires (Tarver et al, 2018). We and others have recently successfully employed MirGeneDB complements in a range of comparative (Fromm et al, 2021; Hu et al, 2021), phylogenetic (Ma et al, 2021; Rosani et al, 2021) and evolutionary studies (Peterson et al, 2022), as a validation cohort for experimental findings (Kang et al, 2021; Baronti et al, 2020), and as a standard reference for the development of novel bioinformatics tools (https://github.com/sinanugur/MirMachine).

### *Variable allometric scaling and stabilizing selection of sMR with respect to mirFam*

For a BM process, between-species trait covariances are proportional to their shared ancestry, and a BM model will be favored if most of the crown species diverged recently relative to the total age represented by the phylogeny, as in the case of the mammalian tree used in this study (Álvarez-Carretero et al, 2022). Furthermore, for a small sample and phylogeny the mvSLOUCH algorithm for the comparison of OU and BM models exhibits a bias towards BM that has been attributed to a difference in the effective population size for each process (Bartoszek, 2016). For example, in a reanalysis of Darwin's data for 13 species of finch (Harmon et al, 2008), two different measures of effective population size yielded correction factors of ~ 0.5 and ~ 0.9 for the BM and OU models, respectively (Bartoszek, 2016). However, even before applying an empirical correction for bias, we

found that an OU process was consistently favored over a BM process for the evolution of *sMR* with respect to *mirFam*, in both the 14-tetrapod and 10-mammal datasets.

We used a maximum likelihood approach to optimize the scaling of *sMR* with respect to *mirFam*, yielding distributions that are homoscedastic (Supplementary Figure S3), as required to compare evolutionary rates across species ranging over orders of magnitude in size (Benson et al, 2022). The optimal slopes obtained by phylogenetic linear regression for the dependence of *sMR* on *mirFam* in tetrapods and mammals were $M^{0.68}$ and $M^{0.71}$, respectively (Supplementary Table S2), but the AICc information criteria for both BM and OU models reached their minimal values when *sMR* was scaled to $M^{0.75}$, where BM and OU processes most precisely simulated the biphasic evolution of *sMR* (Supplementary Figure S5). The analogous models with respect to microRNA genes exhibited the same optimum, with similar rate of adaptation for the OU model, but no optimum *sMR* was observed in relation to genome size or number of coding genes (Supplementary Figure S4), indicating that the coevolution of *sMR* and the microRNA complement is specific and related to their mechanism of action.

Three-quarter power scaling corresponds closely to the conserved slope of log *rMR*/log mass reported for mammals in countless reports since Kleiber (1932), Brody and Proctor (1932) (see Introduction for additional references). This observation suggests that the *sMR-mirFam* relationship evolved under constraints similar to those governing overall *MR*, and supports the assumption that *mirFam* is a useful indicator of the impact of global microRNA activity on cellular *MR*. Furthermore, the evidence that the *sMR-mirFam* relationship has been maintained by selection may represent one manifestation of the multivariate selection on *rMR* and *M* (White et al, 2019), and demonstrates the value of the maximum likelihood approach for analysis of the evolution of the *rMR*/*M* ratio in relation to a third covariate.

### *An adaptive shift at the divergence of Boreoeutheria simulates the evolution of sMR*

The advent of placentation allowed some orders to exploit high quality resources through an increase in energy expenditure and reproductive output, adaptations denied to monotremes and marsupials with access to the same resources (McNab, 2008). Among Boreoeutheria some clades, like Eulipotyphla and Chiroptera, retained the lower body temperatures (≤ 36°C) characteristic of early-branching placentals (Xenarthra and Afrotheria), while others evolved higher $T_b$'s, such as the Carnivora, Artiodactyla, primates and most rodents (Supplementary Figure S2). This divergence in body temperature regimes was associated with differences in the relative prevalence of homeothermy *versus* heterothermy *i.e.* daily torpor. Heterothermy is achieved by lowering the $T_b$ set point, and evolved as an energy-saving strategy in small (< 1 kg) birds and mammals that were reliant on foraging and more vulnerable to changes in the food supply (Ruf and Geiser, 2015). After accounting for mass, climate and geography, early-branching orders exhibit more variable $T_b$ (Boyles et al, 2013), a higher incidence of heterothermy (Ruf and Geiser, 2015), a lower proportion of skeletal muscle mass, and lower *sMR*s,

compared to the majority of late-branching mammals (most orders diverging after Chiroptera), as well as birds, where $T_b$ > 36°C and permanent homeothermy predominate (McNab, 2019).

### *Optimally scaled MRs may also predict the microRNA complement in birds*

The optimal *MR* scaling with respect to *mirFam* in tetrapods ($rMR/M^{0.68}$) or mammals ($rMR/M^{0.71}$) represents a higher than average *MR* per unit mass or volume, as has been predicted for a thermoregulatory core (Scholander et al, 1950; Porter and Kearney, 2009; Speakman and Król, 2010). The greater surface area dependence of *sMR* with respect to *mirFam* may shed light on the correlation between vertebrate morphological patterns and microRNA complement size reported by Deline et al (2018). These authors demonstrated that morphological types were significantly related to the number of microRNA families, but not to genome size or the diversity of protein domains. Furthermore, the morphospace occupied by birds was significantly displaced from a reptilian-mammalian axis (Deline et al, 2018), an interesting parallel to the shift in the optimal *sMR-mirFam* scaling in birds, where *sMR*s are positively related to *mirFam* only when the allometric exponent is set lower than the allometric exponent (0.64) reported for overall *rMR* (Fristoe et al, 2015). This example illustrates an aspect of *MR* scaling that is overlooked when comparing allometric exponents obtained by the power law model, *i.e.* the slope of log *rMR*/log mass: differences in allometric exponents most often represent shifts in the rank order of the ratios between *sMR* and a third covariate. For example, in the sample of 10 mammals included in this study, the dog has the highest ratio of *sMR*/*mirFam* when *sMR* is scaled to $M^{0.70}$, third highest at $M^{0.75}$ and fourth lowest at $M^{0.80}$.

Furthermore, there is an important difference between birds and mammals in the regulatory context in which microRNAs operate. Ancestral birds underwent a reduction in genome size, from *c.* 2 Gb to *c.* 1 Gb, primarily by jettisoning transposable elements (TEs). The massive loss of TEs in the ancestral avian genome contrasts with the steady evolutionary accumulation of TEs in mammals, where they occupy 40 - 50% of the genome (Zhang et al, 2014a; Kapusta et al, 2017; Platt et al, 2018). Retrotransposon sequences have been identified in the 3'- UTRs of 25% of mammalian coding genes, where they serve as binding sites for inhibitory KRAB-ZnF transcription factors (Faulkner et al, 2009). The loss of TEs in the ancestral bird genome was accompanied by the nearly complete loss of KRAB-ZnFs (Liu et al, 2014; Imbeault et al, 2017), implicating microRNA activity as the primary mechanism for the downregulation of gene expression in birds. Like the compact genome and lack of a KRAB-TE apparatus, a reduced microRNA complement and a shift, relative to mammals, in the setpoint for *sMR-mirFam* relationship (this study), may represent adaptations related to the evolution of endothermy and flight.

### *A working model for the evolution of cellular MR in relation to mirFam*

The demonstration that the *sMR* distribution in mammals was best simulated by an adaptive shift at the divergence of Boreoeutheria, and its implication of a Simpsonian jump (Simpson, 1994), suggests a model with distinct adaptive optima for low- and high-$T_b$ mammals. Figure 6 illustrates estimated temperature gradients and optimal *sMR* scaling for linear regression on *mirFam* in early- and late-branching mammals (Supplementary Table S2). A separate optimum is shown for birds, corresponding to the clustering of bird $T_b$'s around 39.8°C (2.66% coefficient of variation, n = 211) and an allometric exponent shifted below the slope of log *rMR*/log mass in birds (0.64) (Fristoe et al, 2015).

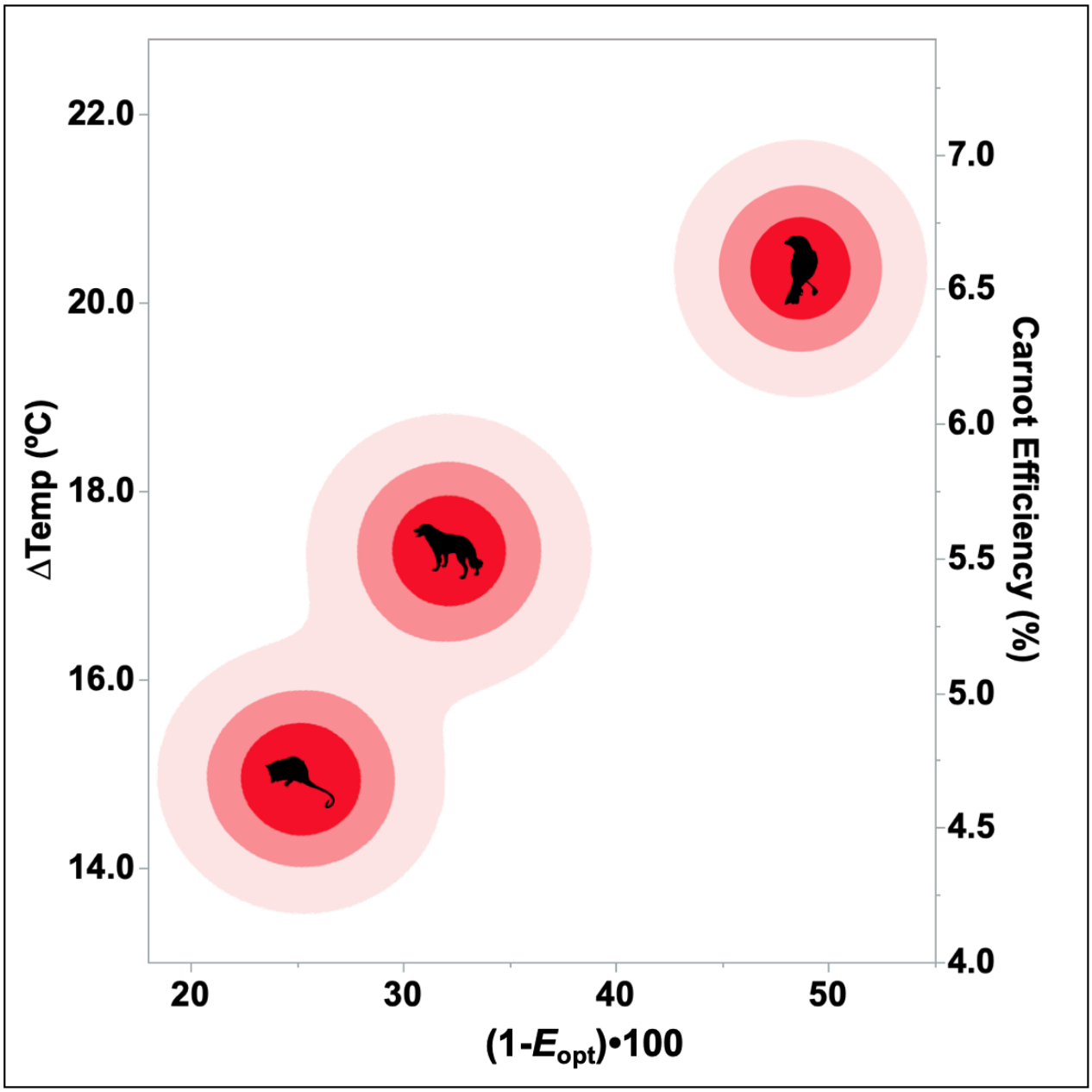


**Figure 6**. Contour plot of a hypothetical fitness landscape for the optimal *sMR* scaling with respect to the number of microRNA families against a hypothetical core-surface temperature gradient. *Eopt*: optimal allometric exponent for fitting *sMR* to the number of microRNA families. ΔTemp = $T_b$ - 20°C. Silhouettes represent early- and late-branching mammals and birds (Phylophic © 2019).

The Carnot efficiency is provided for each hypothetical temperature gradient: for example, there is a theoretical 2% difference in thermodynamic efficiency between birds and early-branching mammals, based on the same ambient temperature (Figure 6), potentially offsetting some of the energy cost of sustaining higher body temperatures. As previously noted, the predicted number of microRNA target sites per coding gene increased approximately 4-fold in the mammalian lineage (Agarwal et al, 2015), while the number of shared microRNA genes and families increased twofold, suggesting a fitness benefit related to the overall number of microRNA-target interactions. Since the majority of mammalian-specific target sites appear to be evolving neutrally (Simkin et al, 2020), such interactions, while appearing to be phenotypically silent, could in theory provide an immediate energy-saving benefit.

The inference of distinct adaptive peaks is based on the currently available mammalian microRNA repertoires in MirGeneDB (Fromm et al, 2020) which represent only two of the four possible combinations of ancestry and phenotype: early-branching mammals with low $T_b$'s and late-branching mammals with high $T_b$'s. The addition of definitive microRNA repertoires to intermediate branches of the mammalian tree, such as those of low $T_b$ Chiroptera, may eventually bridge these hypothetical optima, in which case a genetic drift model might account for the observed variation better than a process of stabilizing selection. On the other hand, the evolution of $T_b$ across 554 mammals has been found to be relatively static when compared to the rates of change of *MR* and ambient temperature (Avaria-Llautureo et al, 2019), consistent with an adaptive barrier to the emergence of higher $T_b$'s. As mammals diversified in size (and ratio of surface area to mass) in response to cooler environments (Clavel and Morlon, 2017; Avaria-Llautureo, 2019), multiple anatomic and physiological mechanisms were available to adjust overall *MR* without altering $T_b$ or cellular *MR*, including changes in thermal conductance (Fristoe et al, 2015) and relative organ size (Wang et al, 2012), particularly that of skeletal muscle (Rowland et al, 2015; McNab, 2019; Wright et al, 2021). However, shifting to a higher $T_b$ and cellular *MR* while maintaining the strict relationship between size and rate of protein synthesis during the cell cycle would have depended on the ability to synchronize the expression of hundreds of regulatory genes and the activities of their target pathways. Just such a role has been proposed for microRNAs: microRNAs were essential to the buffer the effect of temperature fluctuation on photoreceptor development in Drosophila (Li et al, 2009), and when the metabolic rate of fruit flies was genetically engineered to be slower, doubling the time to eclosion, the entire microRNA repertoire was rendered dispensable for normal development (Cassidy et al, 2019). Thus, the eukaryotic ancestry of the mechanisms coordinating growth in cell size and rate of protein synthesis (Knapp et al, 2019; Neurohr et al, 2019), and its evident constraint on the range of cellular *MR* in mammals, suggest that the evolution of higher $T_b$'s and permanent homeothermy may have depended on the ability of microRNAs to synchronize regulatory mechanisms with cellular metabolic rates.

The adaptive value of repression by individual microRNAs operating in gene regulatory networks has been attributed to their ability to canalize phenotype expression by buffering the effects of environmental or allelic variation (Hornstein and Shomron, 2006; Li et al, 2009; Cassidy et al, 2013), to set thresholds for cell fate determination (Mukherji et al, 2011; Ebert and Sharp, 2012), and to mediate the covariation of functionally-related proteins (Tarbier et al, 2020). In bilateral animals, the ability of each microRNA seed to regulate many targets may have facilitated the evolution of regulatory networks of increasing complexity (Moran et al, 2017). Given potential for microRNA regulation to increase the heritability of adaptive traits (Peterson et al, 2009), the enlargement of microRNA and target repertoires has been proposed as a key mechanism for the diversification of animal cell types and morphologies (Makeyev and Maniatis, 2008; Erwin et al, 2011; Deline et al, 2018; Dexheimer and Cochella, 2020; Peterson et al, 2021).

On the other hand, the nature of global microRNA activity and its impact on energy metabolism has received relatively little attention (Schwanhäusser et al, 2011; Cassidy et al, 2019; Tarbier et al, 2020). Given the high metabolic cost of protein synthesis and its strict relationship to cell size (Ginzberg et al, 2018; Björklund, 2019), we have explored the covariation of cellular *MR* and the size of the microRNA complement using variable allometric scaling and the simulation of stabilizing selection. The evolution of cellular *MR* in mammals appears to have been characterized by rapid adaptation in relation to the number of microRNA families. Whatever the ultimate cause of the steady acquisition of microRNA families in vertebrates (Peterson et al, 2021), these observations support a role for global microRNA activity in maintaining metabolic efficiency, potentially facilitating an adaptive shift among late-branching mammals to higher body temperatures, metabolic rates, and permanent homeothermy.

## DATA AVAILABILITY

The original data for all analyses and the results of phylogenetic regressions are provided in Tables S1 and S2 in the Supplementary Information. Phylogenetic tree matrices are available upon request.

## ACKNOWLEDGMENT

BF is supported by the Tromsø forskningsstiftelse (TFS) [20_SG_BF ‘MIRevolution’].

## AUTHOR CONTRIBUTIONS

Conceptualization: BF and TS; Methodology: TS; Investigation: BF and TS; Writing – Original Draft: TS; Writing – Review & Editing: BF and TS; Visualization: BF and TS; Funding Acquisition: BF.

## DECLARATION OF INTERESTS

The authors declare no competing interests.

## METHODS

### *microRNA Families, Genes and Targets, and other genomic variables*

The numbers of conserved microRNA families and genes for 20 vertebrate species were obtained from MirGeneDB, a curated database of microRNA-encoding genes (Fromm et al, 2020). Conserved microRNAs are those shared by two or more species: the species used herein are phylogenetically distinct enough to make this definition valid and workable. The number of conserved mammalian mRNA targets was extracted from the TargetScan8.0 database (Agarwal et al, 2015; McGeary et al, 2019). Values for the other genetic variables (genome size and number of coding genes) were obtained from the NCBI genome assembly database (as of March, 2022).

### *Resting Metabolic Rates and Temperature Correction*

Rates of oxygen consumption and body temperature were drawn primarily from the compilations of White et al (2006) and Gillooly et al (2017). Where multiple values had been recorded at different temperatures, we used the value nearest to the standard body temperature (see below). The original reference for each species is listed in Table S1 of the Supplementary Information. Resting metabolic rates (*rMR*s) were corrected to 38˚C for endotherms, and 25˚C for ectotherms, as *per* White et al (2006) and Gillooly et al (2017). Since oxygen consumption data were available only for *X. laevis*, and *X. tropicalis* adults are approximately half the size of adult *X. laevis*, we assumed 0.54 the *rMR* of *X. laevis* (assuming $rMR_2/rMR_1 = M_2^{0.88}/M_1^{0.88}$ for amphibia).

### *Phylogenies*

Phytools was used to generate a 20-species vertebrate tree and phenogram, 14-species tetrapod tree and 10-species mammalian tree (Revell, 2012) based on divergence times drawn from Álvarez-Carretero et al (2022) for mammals, and Irisarri et al (2017) for earlier-branching vertebrates. Trees were made ultrametric and scaled to unit height using Mesquite © (2021).

In order to model the evolution of the number of microRNA families, a matrix of interspecific distances was assembled based on the number of conserved microRNA families (MirGeneDB: March, 2022) (Fromm et al, 2020), without considering losses or gains unique to each lineage. A distance tree was inferred by minimal evolution (LeFort et al, 2015).

### *Statistics*

Phylogenetic linear regression was carried out using the *R: CAPER* package (Orme, 2013) using the maximum likelihood estimate between 0.0-1.0 for the *lambda* parameter (Pagel, 1999). A value of 1.0 indicates that the observed variation in phenotype conforms to a Brownian motion model of trait evolution, mirroring phylogenetic distance, while a value of 0.0 implies phylogeny-independent trait

evolution, equivalent to a star phylogeny (Felsenstein, 1985; Pagel, 1999; Revell, 2010). All $R^2$ values were adjusted for the number of predictors.

Multivariate correlations, ANCOVA and ordinal logistic regression were performed in JMP®16. For analysis of the fold variation by quintile in cellular *MR*, Chiroptera and 21 outliers (*sMR*68, Cauchy robust fit) were removed from the original dataset of Clarke et al (2010), leaving 532 species. Like other ruminants, the cow was considered an outlier with respect to *MR* (White and Seymour, 2005). All other statistical tests were performed in R (2020).

### *OU versus BM comparison and simulation*

BM and OU models of the optimal *sMR* with respect to *mirFam* were evaluated with the package mvSLOUCH (Bartoszek et al, 2012), with six repetitions of the hill-climbing algorithm for the OU process with two adaptation matrices (Diagonal and DecomposableReal). Preliminary validation based on the AICc criterion revealed that for the 14 tetrapod model, OU processes were misclassified as BM for 50% of the simulations, while 10% of the BM simulations were misclassified as OU. The corresponding rates of misclassification for the 10 mammal model were 75% and 5% (n = 40, Supplementary Table S3). The rates of correct classification for the BM and OU simulations were equalized by adjusting the AICc scores +/- 2.1 for the tetrapod model, or +/- 4.0 for the mammalian model (Supplementary Table S3).

The Phylogenetic EM package (Bastide et al, 2018) was used to simulate *sMR* and *mirFam* distributions using variance/covariance matrix for *sMR*75 on *mirFam* as the selection strength matrix, with the median setting (3) for selection strength (Supplementary Figure S3). The average mammalian values for *sMR*75 and *mirFam* were assigned to the first adaptive shift (divergence of mammals), and the corresponding placental averages were assigned to the second adaptive shift (divergence of Atlantogenata or Boreoeutheria or Euarchontoglires) (see Figure 5A). Ten simulations were generated and averaged for each shift or pair of shifts.

REFERENCES

Agarwal V, Bell GW, Nam J, Bartel DP. 2015. Predicting effective microRNA target sites in mammalian mRNAs. *eLife* 4: e05005.

Álvarez-Carretero S, Tamuri A, Battini M, Nascimento F, Carlisle E, Asher R, Yang Z, Donoghue P and Dos Reis M. 2022. A species-level timeline of mammal evolution integrating phylogenomic data. *Nature* 602: 263-267.

Avaria-Llautureo J, Hernandez CE, Rodriguez-Serrano E and Venditti, C. 2019. The decoupled nature of basal metabolic rate and body temperature in endotherm evolution. *Natur*e 572: 651-654.

Axtell MJ and Meyers BC. 2018. Revisiting criteria for plant microRNA annotation in the era of big data. *Plant Cell* 30: 272-284.

Baek D, Villén J, Shin C, Camargo FD, Gygi SP and Bartel DP. 2008. The impact of microRNAs on protein output. *Nature* 455: 64-72.

Ballesteros FJ, Martinez VJ, Luque B, Lacasa L, Valor E and Moya A. 2018. On the thermodynamic origin of metabolic scaling. *Scientific Reports* 8: 1448.

Banerjee K, Kolomeisky AB and Igoshin OA. 2017. Elucidating interplay of speed and accuracy in biological error correction. *PNAS* 114: 5183-5188.

Barato AC and Seifert U. 2015. Thermodynamic uncertainty relation for biomolecular processes. *Phys Rev Lett* 114: 158101.

Baronti L, Guzzetti I, Ebrahimi P, Sandoz SF, Steiner E, Schlagwitneit J, Fromm B, Silva L, Fontana C, Chen AA and Petzold K. 2020. Base-pair conformational switch modulates miR-34a targeting of Sirt1 mRNA. *Nature* 583: 139-144.

Bartel DP. 2018. Metazoan MicroRNAS. *Cell* 173: 20-51.

Bartel DP and Chen CZ. 2004. Micromanagers of gene expression: the potentially widespread influence of metazoan microRNAs. *Nature Genet* 5: 396-400.

Bartoszek K. 2016. Phylogenetic effective sample size. *J Theor Biol* 4017: 371-386.

Bartoszek K, Pienaar J, Mostad P, Andersson S and Hansen TF. 2012. A phylogenetic comparative method for studying multivariate adaptation. *J Theor Biol* 314: 204-215.

Bastide P, Mariadassou M and Robin S. 2018. Detection of adaptive shifts on phylogenies by using shifted stochastic processes on a tree. *J R Stat Soc B 79*: 1067-1093.

Bennett CH. 1979. Dissipation-error tradeoff in proofreading. *Biosystems* 11: 85-91.

Benson RBJ, Godoy P, Bronzati M, Butler RJ and Gearty W. 2022. Reconstructed evolutionary patterns for crocodile-line archosaurs demonstrate impact of failure to log-transform body size data. *Communications Biology* 171: 1-4.

Björklund M. 2019. Cell size homeostasis: Metabolic control of growth and cell division. *BBA Mol Cell Res* 1866: 409-417.

Boyles JG, Thompson AB, McKechnie AE, Malan E, Humphries MM and Careau. 2013. A global heterothermic continuum in mammals. *Global Ecol Biogeogr* 22: 1029-1039.

Brody S and Proctor RC. 1932. Relation between basal metabolism and mature body weight in different species of mammals and birds. *Univ Missouri Agr Exp Stn Res Bull* 166: 89–101.

Buttgereit F and Brand MD. 1995. A hierarchy of ATP-consuming processes in mammalian cells. *Biochem J* 312: 163-167.

Cassidy JJ, Bernasek SM, Bakker R, Giri R, Peláez, N, Eder B, Bobrowska A, Bagheri N, Amaral LAN and Carthew RW. 2019. Repressive gene regulation synchronizes development with cellular metabolism. *Cell* 178: 1-13.

Cassidy JJ, Jha JR, Posadas DM, Giri R, Venken KJT, Ji J, Jiang H, Bellen HJ, White KP and Carthew RW. 2013. miR-9a Minimizes the Phenotypic Impact of Genomic Diversity by Buffering a Transcription Factor. *Cell* 155: 1556-1567.

Castellano L and Stebbing J. 2013. Deep sequencing of small RNAs identifies canonical and non-canonical microRNA and endogenous siRNAs in mammalian somatic tissues. *Nucl Acid Res* 41: 3339-3351.

Chiang HR, Schoenfeld LW, Ruby JG, Auyeung VC, Spies N, Baek D, Johnston WK, Russ C, Luo S, Babiarz JE et al. 2010. Mammalian microRNAs: experimental evaluation of novel and previously annotated genes. *Genes Dev* 24: 992-1009.

Choi IY, Kwon EC and Kim NS. 2020. The C- and G-value paradox with polyploidy, repeatomes, introns, phenomes and cell economy. *Genes Genomics*: 699-714.

Clarke A, Rothery P and Isaac NJP. 2010. Scaling of basal metabolic rate with body mass and temperature in mammals. *J Animal Ecol* 79: 610-619.

Clavel J and Morlon H. 2017. Accelerated body size evolution during cold climatic periods in the Cenozoic. *PNAS* 114: 4183-4188.

Deline B, Greenwood JM, Clark JW, Puttick MN, Peterson KJ, Donoghue PCJ. 2018. Evolution of metazoan morphological disparity. *PNAS* 29: E8909-E8918.

Dexheimer PJ and Cochella L. 2020. MicroRNAs: from mechanism to organism.
*Frontiers in Cell and Dev Biol* 8: 409.

Ebert MS and Sharp PA. 2012. Roles for MicroRNAs in conferring robustness to biological processes. *Cell* 149: 515-524.

Erwin DH, Laflamme M, Tweedt SM, Sperling EA, Pisani D and Peterson KJ. 2011. The Cambrian conundrum: early divergence and later ecological success in the early history of animals.
*Science* 334: 1091-1097.

Faulkner GF, Kimura Y, Daub CO, Wani S, Plessy C, Irvine KM, Schroder K et al. 2009. The regulated retrotransposon transcriptome of mammalian cells. *Nature Genet* 41: 563-571.

Felsenstein J. 1985. Phylogenies and the comparative method. *American Naturalist* 125: 1-15.

Friedman RC, Farh KKH, Burge CB and Bartel DP. 2009. Most mammalian mRNAs are targets of microRNAs. *Genome Res* 19: 92-105.

Fristoe TS, Burger JR, Balk MA, Khaliq I, Hof C and Brown JH. 2015. Metabolic heat production and thermal conductance are mass-independent adaptations to the thermal environment in birds and mammals. *PNAS* 112: 15934-15939.

Fromm B, Billipp T, Peck LE, Johansen M, Tarver JE, King BL, Newcomb JM, Sempere LF, Flatmark K, Hovig E and Peterson KJ. 2015. A uniform system for the annotation of vertebrate microRNA genes and the evolution of the human microRNAome. *Ann Rev Genet* 49: 213-242.

Fromm N, Domanska F, Høye F, Ovchinnikov V, Kang E, Aparicio-Puerta R, Johansen M, Flatmark K, Mathelier A, Hovig E, Hackenberg M, Friedländer MR and Peterson KJ. 2020. MirGeneDB 2.0: The metazoan microRNA complement. *Nucl Acids Res* 48: D132–D141.

Fromm B, Høye E, Domanska D, Zhong X, Aparicio-Puerta E, Ovchinnikov V, Umu SU, Chabot, PJ, Kang W, Aslanzadeh M, Tarbier M, Mármol-Sánchez E, Urgese G, Johansen M, Hovig E, Hackenberg M, Friedländer MR and Peterson KJ. 2021. MirGeneDB 2.1: toward a complete sampling of all major animal phyla. *Nucl Acids Res* 50: D204-D210.

Fromm B, Tarbier M, Smith O, Mármol-Sánchez E, Dalén L, Gilbert MTP and Friedländer MR. 2021. Ancient microRNA profiles of 14,300-yr-old canid samples confirm taxonomic origin and provide glimpses into tissue-specific gene regulation from the Pleistocene. *RNA* 27: 324-334.

Gillooly JF, Gomez JP and Mavrodiev EV. 2017. A broad-scale comparison of aerobic activity levels in vertebrates: endotherms versus ectotherms. *Proc R Soc B* 284: 20162328.

Ginzberg MB, Chang N, D'Souza H, Patel N, Kafri R and Kirschner MW. 2018. Cell size sensing in animal cells coordinates anabolic growth rates and cell cycle progression to maintain cell size uniformity. *elife* 7: e26957.

Harmon LJ, Weir JT, Brock CD, Glor RE and Challenger W. 2008. GEIGER: investigating evolutionary radiations. *Bioinformatics* 24: 129–131.

Hopfield JJ. 1974. Kinetic proofreading: A new mechanism for reducing errors in biosynthetic processes requiring high specificity. *PNAS* 71: 4135-4139.

Hornstein H and Shomron N. 2006. Canalization of development by microRNAS.
*Nature Genetics* 38: S20-S24.

Hu RS, Zhang XX, Ma QN, Elsheika HM, Ehsan M, Zhao Q, Fromm B and Zhu XQ. 2021. Differential expression of microRNAs and tRNA fragments mediate the adaptation of the liver fluke Fasciola gigantica to its intermediate snail and definitive mammalian hosts. *Int J Parasitol* 51: 405-414.

Imbeault M, Helleboid PY and Trono D. 2017. KRAB zinc-finger proteins contribute to the evolution of gene regulatory networks. *Nature* 543: 550-554.

Irisarri I, Baurain D, Brinkmann H, Delsuc F, Sire JY, KupferA, Petersen J, Jarek M, Meyer A, Vences M, and Philippe H. 2017. Phylotranscriptomic consolidation of the jawed vertebrate timetree. *Nature Ecol Evol* 1: 1370-1378.

Jones-Rhoades MW. 2012. Conservation and divergence in plant microRNAs. *Plant Mol Biol* 80: 3-16.

Kafri M, Metzi-Raz E, Jonas F and Barkai N. 2016. Rethinking cell growth models.
*FEMS Yeast Research* 16: fow081

Kang W, Fromm B, Houben AJ, Høye E, Bezdan D, Arnan C, Thrane K, Asp M, Johnson R, Biryukova I and Friedländer MR. 2021. MapToCleave: High-throughput profiling of microRNA biogenesis in living cells. *Cell Rep* 37: 110015.

Kapusta A, Suh A and Feschotte. 2017. Dynamics of genome size evolution in birds and mammals. *PNAS* 114: E1460-E1469.

Kleiber M. 1932. Body size and metabolism. *Hilgardia* 6: 315-353.

Knapp BD, Odermatt P, Rojas ER, Cheng W, He X, Huang KC and Chang F. 2019. Decoupling of Rates of Protein Synthesis from Cell Expansion Leads to Supergrowth. *Cell Systems* 9: 434-445.

Koteja P. 2000. Energy assimilation, parental care and the evolution of endothermy.
*Proc R Soc B*. 267: 479-484.

Krek A, Grün D, Poy MN, Wolf R, Rosenberg L, Epstein EJ, MacMenamin P, de Piedade I, Gunsalus KC, Stoffel M and Rajewsky N. 2005. Combinatorial microRNA Predictions. *Nature Genetics* 37: 495-500.

Langenberger D, Bartschat S, Hertel J, Hoffmann S, Tafer H and Stadler PF. 2011. MicroRNA or not microRNA? Advances in Bioinformatics and Computational Biology.
pp 1-9. Springer (Berlin, Heidelberg).

Lefort V, Desper R and Gascuel O. 2015. A comprehensive, accurate and fast distance-based phylogeny inference program. *Mol Biol Evol* 32: 2798-800.

Li X, Cassidy JJ, Reinke CA, Fischboeck S and Carthew RW. 2009. A microRNA imparts robustness against environmental fluctuation during development. *Cell* 137: 273-282.

Lin J and Amir A. 2018. Homeostasis of protein and mRNA concentrations in growing cells. *Nature Comm* 9: 4496.

Lin J and Amir A. 2021. Disentangling intrinsic and extrinsic gene expression noise in growing cells. *Phys Rev Lett* 126: 078101

Liu H, Chang LH, Sun Y, Lu X and Stubbs L. 2014. Deep vertebrate roots for mammalian zinc finger transcription families. *Genome Biol Evol* 6: 510-525.

Ludwig N, Becker M, Schumann T, Speer T, Fehlmann T, Keller A and Meese B. 2017. Bias in recent miRBase annotations potentially associated with RNA quality issues. *Sci Rep* 7: 5162.

Lynch M and Marinov GK. 2015. The bioenergetic costs of a gene. *PNAS* 112: 15690-15695.

Ma X, He K, Shi Z, Li M, Li F and Chen XX. 2021. Large-Scale Annotation and Evolution Analysis of microRNA in Insects. *Genome Biol Evol* 13: evab083.

Maino JL, Kearney MR, Nisbet RM and Kooijman SALM. 2014. Reconciling theories for metabolic scaling. *J Animal Ecol* 83: 20-29.

Makeyev EV and Maniatis T. 2008. Multilevel Regulation of Gene Expression by MicroRNAs. *Science* 319: 1789-1790.

Mallory JD, Kolomeisky AB and Igoshin OA. 2019. Trade-offs between error, speed, noise, and energy dissipation in biological processes with proofreading. *J Phys Chem B* 123: 4718-4725.

McGeary SE, Lin KS, Shi CY, Pham TM, Bisaria N, Kelley GM and Bartel DP. 2019. The biochemical basis of microRNA targeting efficacy. *Science* 366: eaav1741.

McNab BK. 2008. An analysis of the factors that influence the level and scaling of mammalian BMR. *Comp Biochem Physiol A* 151, 5-28.

McNab BK. 2009. Ecological factors affect the level and scaling of avian BMR.

*Comp Biochem Physiol A* 152: 22-45.
McNab BK. 2019. What determines the basal rate of metabolism? *J Exp Biol* 222: jeb205591.

Meng Y, Shao C, Wang H and Chen M. 2012. Are all the miRBase-registered microRNAs true? A structure- and expression-based re-examination in plants. *RNA Biol* 9: 249-253.

Moran Y, Agron M, Praher D and Technau U. 2017. The evolutionary origin of plant and animal microRNAs. *Nature Ecol Evol* 1: 0027.

Mukherji S, Ebert MS, Zheng GXY, Tsang JS, Sharp PA and van Oudenaarden A. 2011. MicroRNAs can generate thresholds in target gene expression. *Nature Genetics* 43: 854-859.

Naya DE, Spangenberg L, Naya H and Bozinovic F. 2013. How does evolutionary variation in metabolic rate arise? A statistical assessment and a mechanistic model. *Evolution* 67: 1463-1476.

Neurohr GE, Terry RL, Lengefeld J et al. 2019. Excessive Cell Growth Causes Cytoplasm Dilution And Contributes to Senescence. *Cell* 176: 1083-1097.

Ninio J. 1975. Kinetic amplification of enzyme discrimination. *Biochimie* 57: 587-595.

Orme D, Freckleton RP, Thomas GH and Petzoldt T. 2013. CAPER: comparative analyses of phylogenetics and evolution in R. *Methods Ecol and Evol* 3: 141-151.

Ozbudak EM, Thattai M, Kurtser I, Grossman AD and van Oudenaarden. 2002. Regulation of noise in the expression of a single gene. *Nature Genetics* 31: 69-73.

Pagel M. 1999. Inferring the historical patterns of biological evolution.
*Nature* 401: 877-884.

Peterson KJ, Dietrich MR and McPeek, MA. 2009. MicroRNAs and metazoan macroevolution: insights into canalization, complexity, and the Cambrian explosion. *BioEssays* 31: 736–747.

Peterson KJ, Beavan A, Chabot PJ, McPeek MA, Pisani D, Fromm B and Simakov O. 2022. MicroRNAs as Indicators into the Causes and Consequences of Whole-Genome Duplication Events. *Mol Biol Evol* 39: msab344.

Platt RN, Vandewege MW and Ray DA. 2018. Mammalian transposable elements and their impacts on genome evolution. *Chromosome Res* 26:25–43.

Porter WP and Kearney M. 2009. Size, shape, and the thermal niche of endotherms. 2009. *PNAS* 106: 19666–19672.

R Core Team. 2020. R: a language and environment for statistical computing. R Foundation for Statistical Computing. Vienna, Austria.

Revell LJ. 2010. Phylogenetic signal and linear regression on species data.
*Methods Ecol Evol* 1: 319-329.

Revell LJ. 2012. phytools: an R package for phylogenetic comparative biology
(and other things). *Methods Ecol Evol* 3: 217–223.

Rolfe DF, and Brown GC. 1997. Cellular energy utilization and molecular origin of standard metabolic rate in mammals. *Physiol Rev* 77: 731-58.

Rosani U, Bortoletto E, Bai CM, Novoa B, Figueras A, Venier P and Fromm B. 2021. Digging into bivalve microRNAomes: between conservation and innovation. *Philos Trans R Soc B* 376:20200165.

Rowland LA, Bal NC, Periasamy M. 2015. The role of skeletal-muscle-based thermogenic mechanisms in vertebrate endothermy. *Biol Rev Camb Philos Soc* 90:1279-97.

Ruf T and Geiser F. 2015. Daily torpor and hibernation in birds and mammals.
*Biol Reviews* 90: 891-926.

Savage, VM, Gillooly JF, Woodruff, WH, West GB, Allen AP, Enquist BJ and Brown AC. 2004. The predominance of quarter-power scaling in biology. *Funct Ecol* 18: 257–282.

Schmiedel JM, Klemm SL, Zheng Y, Sahay A, Blüthgen N, Marks DS and van Oudenaarden A. 2015. MicroRNA control of protein expression noise. *Science* 348: 128-132.

Schmiedel JM, Carey LB and Lehner B. 2019. Empirical mean-noise fitness landscapes reveal the fitness impact of gene expression noise. *Nature Comms* 10: 3180.

Scholander PF, Hock R, Walters V, Johnson F and Irving L. 1950. Heat regulation in some arctic and tropical mammals and birds. *Biol Bull* 99: 237-258.

Schwanhäusser B, Busse D, Li N, Dittmar G, Schuchhardt J, Wolf J, Chen W and Selbach M. 2011. Global quantification of mammalian gene expression control. *Nature* 473: 337–342.
Selbach M, Schwanhäusser B, Thierfelder N, Fang Z, Khanin R, Rajewsky N. 2008. Widespread changes in protein synthesis induced by microRNAs. *Nature* 455: 58–63.

Simkin A, Geissler R, McIntyre ABR, and Grimson A. 2020. Evolutionary dynamics of microRNA target sites across vertebrate evolution. *PLoS Genetics* 16: e1008285.

Simpson GG. 1944. Tempo and Mode in Evolution. Columbia University Press. New York.

Speakman JR and Król E. 2010. Maximal heat dissipation capacity and hyperthermia risk: neglected key factors in the ecology of endotherms. *J Anim Ecol* 79: 726–746.

Swanson DL, McKechnie AE and Vézina F. 2017. How low can you go? An adaptive energetic framework for interpreting basal metabolic rate variation in endotherms.
*J Comp Physiol B* 187: 1039-1056.

Tarbier M, Mackowiak SD, Frade J, Catuara-Solarz S, Biryukova I, Gelali E, Menéndez DB, Zapata L, Ossowski S, Bienko M, Gallant CJ, and Friedländer MR. 2020. Nuclear gene proximity and protein interactions shape transcript covariations in mammalian single cells. *Nature Comms* 11: 5445.

Tarver JE, Sperling EA, Nailor A, Heimberg AM, Robinson JM, King BL, Pisani D, Donoghue PCJ and Peterson KJ. 2013. microRNAs: Small Genes with Big Potential in Metazoan Phylogenetics.
*Mol Biol Evol* 30: 2369-2382.

Tarver JE, Taylor RS, Puttick MN, Lloyd GT, Pett W, Fromm B, Schirrmeister BE, Pisani D, Peterson KJ and Donoghue PCJ. 2018. Well-annotated microRNAomes do not evidence pervasive microRNA loss. *Genome Biol Evol* 10: 1457-1470.

Taylor RS, Tarver JE, Hiscock SJ and Donoghue PC. 2014. Evolutionary history of plant microRNAs. *Trends Plant Sci* 19: 175-182.

Thattai M and van Oudenaarden A. 2001. Intrinsic noise in gene regulatory networks.
*PNAS* 98: 8614-8619.

Thompson RC, Plachetzki DC, Mahler DL, Moore BR. 2014. A critical appraisal of the use of microRNA data in phylogenetics. *PNAS* 111: E3659–3668.

Vogel C, Abreu R, Ko D, Le S, Shapiro BA, Burns SC, Sandhu D, Boutz DR, Marcotte EM and Penalva LO. 2010. Sequence signatures and mRNA concentration can explain two- thirds of protein abundance variation in a human cell line. *Mol Syst Biol* 6: 400.

Wagner A. 2005. Energy Constraints on the Evolution of Gene Expression.
*Mol Biol Evol* 22: 1365–1374.

Wang X and Liu XS. 2011. Systematic curation of miRBase annotation using integrated small RNA high-throughput sequencing data for *C. elegans* and *Drosophila*. *Front Genet* 2: 25.

White CR. 2011. Allometric estimation of metabolic rates in animals.
*Comp Biochem Physiol A* 158: 346-357.

White CR, Marshall DJ, Alton LA, Arnold PA, Beaman JE, Bywater CL, Condon C, Crispin TS, Janetzki A, Pirtle E, Winwood-Smith HS, Angilletta MJ, Chenoweth SF, Franklin CE, Franklin CE, Halsey LG, Kearney MR, Portugal SJ and Ortiz-Barrientos D. 2019. The origin and maintenance of metabolic allometry in animals. *Nature Ecol Evol* 3: 598-603.

White CR, Phillips N and Seymour R. 2006. The scaling and temperature dependence of vertebrate metabolism. *Biol Lett* 2: 125 – 127.

White CR and Seymour RS. 2005. Allometric scaling of mammalian metabolism.
*J Exp Biol* 208: 1611-1619.

Wright T, Davis RW, Pearson HC, Murray M and Sheffield-Moore M. 2021. Skeletal muscle thermogenesis enables aquatic life in the smallest marine mammal. *Science* 373: 223–25.

Yu Q, Kolomeisky AB and Igoshin. 2022. The energy cost and optimal design of networks for biological discrimination. *J Royal Soc Interface* 19: 20210883–83.

Zatulovsky E and Skotheim JM. 2020. On the Molecular Mechanisms Regulating Animal Cell Size Homeostasis. *Trends Genetics* 36: 360-372.

Zhang G, Li C, Li Q et al. 2014. Comparative genomics reveals insights into avian genome evolution and adaptation. *Science* 346: 1311-1320.